

Polarization and polarization induced electric field in nitrides – critical evaluation based on DFT studies

Pawel Strak^{}, Pawel Kempisty^{*}, Konrad Sakowski^{*}, and Stanislaw Krukowski^{*†}*

^{*}Institute of High Pressure Physics, Polish Academy of Sciences, Sokolowska 29/37, 01-142 Warsaw,
Poland

[†]Interdisciplinary Centre for Materials Modeling, Warsaw University, Pawinskiego 5a, 02-106
Warsaw, Poland

ABSTRACT

Density Functional Theory (DFT) calculations were used to evaluate polarity of group III nitrides, such as aluminum nitride (AlN), gallium nitride (GaN) and indium nitride (InN) providing physically sound quantitative measure of polarity of these materials. Two different approaches to polarization of nitride semiconductors were assessed and the conclusions have been used to develop models. It was shown that Berry phase formulation of the electron related polarization component provides a number of various solutions, different for various selection of the simulated volume. The electronic part gives saw-like pattern for polarization. A total number of these solutions, related to well known scaling of the geometric phase, is equal to the number of valence electrons in the system. Summation with similar pattern for ionic part provides several polarization values. Standard dipole density formulation depends on the selection of the simulation volume in periodic continuous way. Using a condition of continuous embedding into the infinite medium, and simultaneously, the zero surface charge representation at crystal boundary provides to physically sound solution. This solution is corresponding to maximal and minimal polarization values and also corresponds to different physical termination of the crystal surfaces, either bare or covered by complementary atoms. This change leads to polarization and electric field reversal. The polarization and related fields in finite size systems were obtained.

Keywords: polarization, polarity, gallium nitride, aluminum nitride, indium nitride, density functional theory

PACS: 61.50.Ah, 81.10.Aj

I. INTRODUCTION

Macroscopic polarization of crystalline materials is physically important property of solids¹. It is direct consequence of the symmetry of a crystalline lattice, which allows for the existence of vector

property, in the point group symmetry of the lattice. It is therefore expected that microscopic definition of the property is formulated, in direct consequence of the atomic lattice structure. Unfortunately typical statement, frequently encountered in textbooks, defining polarization as dipole of a unit cell, divided by its volume, is not correct²⁻⁴. As it was pointed out, so defined quantity depends on the selection of the volume, and as such it could not be used to define the physical property of the matter. This is related to the presence of the surface term, inherently involved in the definition of the polarization as an electric dipole density, which affects its value⁵⁻⁹. A direct modification, such as using of large volume, does not remove this deficiency².

Macroscopic polarization is technically important physical property of pyro- and ferro-electrics, often used in many important technological applications. A natural use of permanent or induced electric dipole could be found in many applications¹⁰.

Another important feature of these substances is existence of electric field in the crystal interior. This may affect functionality of advanced electronic and optoelectronic devices. The built-in electric fields affect energy of quantum states that is known as Stark effect. In addition, strain induced field may contribute to this effect significantly, especially in strained quantum low dimensional structures frequently used in modern devices, built on polar GaN(0001) surface¹¹⁻¹³. The electric field changes energy of quantum states of both types of carriers, electrons and holes, giving rise to phenomenon for long time known as Quantum Confined Stark Effect (QCSE)¹⁴. A mere change of the energy could be either beneficial or harmful to the device application; a really detrimental is spatial separation of electrons and holes that are shuffled to the opposite ends of the quantum well¹⁴⁻¹⁶. Spatial separation reduces overlap of the hole-electron wavefunctions, and lowers their radiative recombination rates, and accordingly, efficiency of optoelectronic devices, both LD's and LED's¹⁷⁻²⁰. The negative influence of QCSE effect may be enhanced by Auger recombination or carrier leakage for high carrier density at high injection currents²¹⁻²⁵. That could lead to decrease of the device efficiency for higher injection currents, the phenomenon nicknamed as "efficiency droop"²⁶.

A harmful influence of QCSE for optoelectronic device is compensated by its beneficial contribution in the case of electronic devices based on two-dimensional electron gas (2DEG), such as field effect transistors (FET's) or molecular sensors. These devices use electric field at AlN/GaN heterostructures, which is stabilized by polarization induced 2DEG. Such devices are characterized by high mobility of electron gas which could be used for construction of fast electronic devices. Also, influence of the field, induced by dipoles of the molecules, presented at the surface, may contribute to the sensitivity of molecular sensors which opens new applications of such devices.

These examples prove that polarization is physical property an increasingly important in technology. Development of nanotechnology will even increase its weight. Therefore several attempts were used to reformulate the problem. One approach was to calculate the change of polarization only⁸. Another is to divide polarization into ionic and delocalized charge. The ionic part may be calculated directly, the delocalized contribution may be obtained using Berry phase formulation²⁻⁷. This

formulation provides the required quantity modulo some factor. In the model presented below we formulate polarization using dipole density with imposing boundary conditions. These conditions allow incorporation of the vacuum in the infinite crystal body and let to avoid generation of surface charge. Thus polarization is determined exactly without any inference from the boundary terms. As it is also presented below, polarization induced electric field in the bulk solid may be determined. That determination is compatible with the selection of the termination surfaces, thus provide base for accounting of the field influence on the properties of optoelectronic and electronic devices.

II. CALCULATION METHODS

In the calculations reported below three different DFT codes were used: commercially available VASP²⁷⁻³⁰ freely accessible SIESTA³⁰⁻³² and commercially accessible Dmol³³. A standard plane wave functional basis set, as implemented in VASP, with the energy cutoff of 29.40 Ry (400.0 eV) was used in all reported simulations. As was shown by Lepkowski and Majewski, it gives good results in precise simulations of GaN properties by VASP code³⁴. The Monkhorst-Pack grid: (7x7x7), was used for k-space integration³⁵. For the Ga, Al, In and N atoms, the Projector-Augmented Wave (PAW) potentials for Perdew, Burke and Ernzerhof (PBE) exchange-correlation functional, were used in Generalized Gradient Approximation (GGA) calculations³⁶⁻³⁸. Gallium 3d and Indium 4d electrons were accounted in the valence band explicitly. The energy error for the termination of electronic self-consistent (SCF) loop was set equal to 10^{-6} . The obtained lattice constants were: GaN - $a = 3.195 \text{ \AA}$ and $c = 5.206 \text{ \AA}$, AlN - $a = 3.112 \text{ \AA}$ and $c = 4.983 \text{ \AA}$, and InN - $a = 3.563 \text{ \AA}$ and $c = 5.756 \text{ \AA}$, which is in good agreement with the experimental data: GaN: $a = 3.189 \text{ \AA}$ and $c = 5.185 \text{ \AA}$, for AlN: $a = 3.111 \text{ \AA}$ and $c = 4.981 \text{ \AA}$ and for InN: $a = 3.537 \text{ \AA}$ and $c = 5.706 \text{ \AA}$.

The second code, SIESTA uses norm conserving pseudopotentials with the numeric atomic orbitals local basis functions that have finite size support, determined by the user³⁰⁻³². The pseudopotentials for Ga, Al, In and N atoms were generated, using ATOM program for all-electron calculations^{39, 40}. Gallium 3d and Indium 4d electrons were included in the valence electron set explicitly and were represented by single zeta basis. For s and p type orbitals quadruple zeta basis set were used. Aluminum atom basis was represented by triple zeta function. Integrals in k-space were performed using 3x3x3 Monkhorst-Pack grid. The minimal equivalent of plane wave cutoff for grid was set to 275 Ry. As a convergence criterion terminating SCF loop, the maximum difference between the output and the input of each element of the density matrix was employed being equal or smaller than 10^{-4} .

For comparison, spontaneous polarization was also calculated using DMol3 commercial program³³. In DMol3 package, full-electron Kohn-Sham eigenvalue problem with periodic boundary conditions (PBC) for wave function is solved using basis of Linear Combination of Atomic Orbitals (LCAO)⁴¹. The double zeta plus polarization (DZP) basis set was applied, so that the required matrix elements are evaluated numerically on the properly chosen grid. For exchange energy, approximation

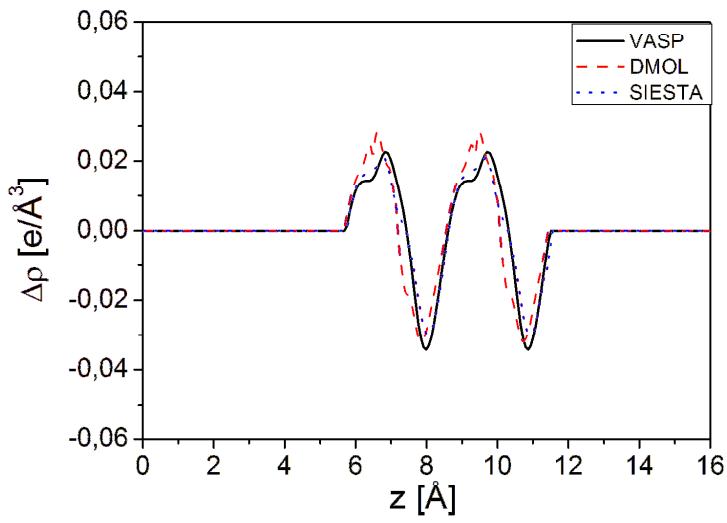
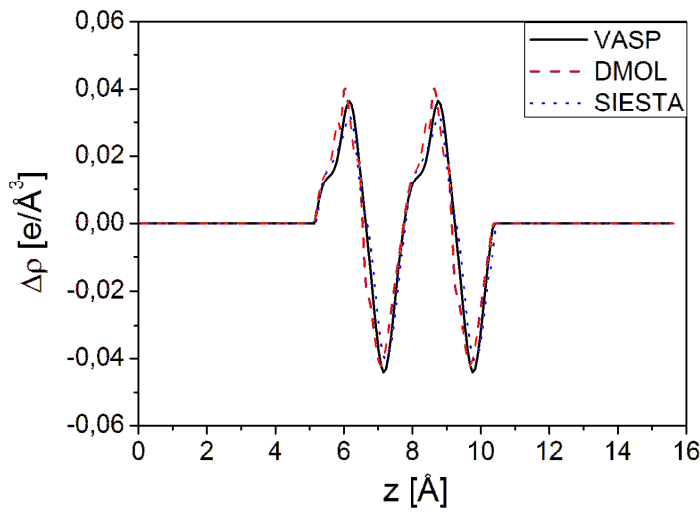
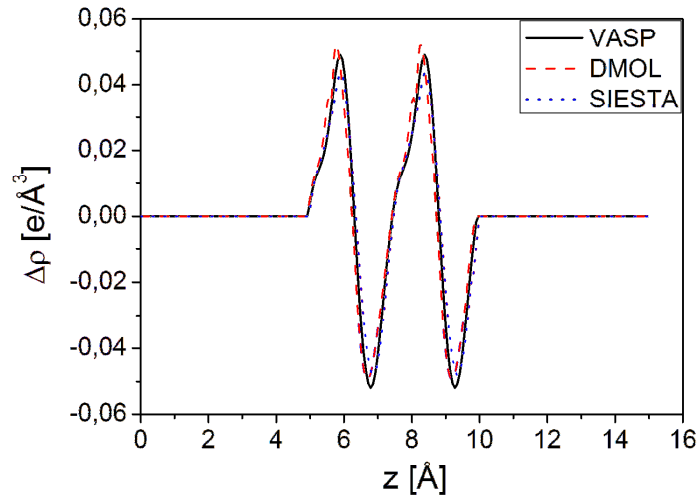
proposed by Becke⁴² and Lee, Yang, Parr⁴³ (B88) was chosen, for correlation energy Tsuneda, Suzumura, Hirao functional was used⁴⁴. The electric potential was determined by solution of Poisson equation which was expressed as sum of the multipole contributions, centered on each atom of the simulated volume with the optimized cutoff radii^{33, 45}. In order to account long range interactions Ewald summation is employed⁴⁶. The method is verified to assure solution tolerance of 10^{-6} hartree. Thus the DMol3 Poisson equation solution procedure is different than that of VASP and SIESTA.

III. DENSITY DISTRIBUTION

The electric fields in VASP and SIESTA are obtained by inverse Fast Fourier Transform (FFT) method where periodicity of electrostatic potentials in the three directions at the edges of the simulated volume is assumed. Such periodicity is enforced by addition of appropriate external field so that any potential changes related to polarization are compensated. DMol3 solution is based on multipole expansion method, employing Ewald summation procedure to account long range interaction. Since the DMol3 wavefunctions basis, are spherical harmonics, that are perfect electric multipoles, the summation employs wavefunction coefficients directly, assuring extremely fast convergence of the Poisson equation solution procedure. Siesta uses both FFT method and molecular orbitals basis set while VASP is combination of FFT and planewave basis set. In order to verify these three approaches the solution from three different methods and basis sets in Kohn-Sham equation are compared. In FIG. 1 the averaged density profiles were presented for AlN, GaN and InN, respectively. The diagrams presents the density difference between densities obtained by full solution of DFT Kohn-Sham equation ρ_{KS} and the sum of densities of separated atoms ρ_{SAO} , averaged in the plane perpendicular to c-axis:

$$\Delta\rho \equiv \rho_{KS} - \rho_{SAO} \quad (1)$$

Naturally, the superposition of charge of separated atoms has no electric dipole moment, therefore this density difference may be used for standard calculation of the polarization and polarization induced electric field. In principle the results should be exactly the same as for electronic and nuclei charge. Some error may arise from intersection of the subtracted separated atom charge (i.e. effectively positive, representing atomic nuclei) by top and bottom boundaries. The coordinate shift, resulting from the periodic boundary conditions may affect magnitude of the dipole obtained from the integration over simulated volume.



(a)

(b)

(c)

FIG. 1. (Color online) Electron density difference of the Kohn-Sham functional and the superposition of atomic charges, plotted along c-axis of single periodic cell with vacuum region added on both sides of: (a) AlN; (b) GaN; (c) InN. The density is averaged in the plane perpendicular to c-axis.

From these diagrams it follows that these solutions are fairly close for all three methods. That indicates on good convergence of the calculations and proper representation of the real density distribution by DFT solution.

Due to periodic boundary conditions, the density distribution should be also periodic. This does not specify exactly the choice of the simulated volume as its boundaries can be selected arbitrarily. Since the simulated system is electrically neutral, integral over the density should vanish, thus there are at least two different locations of the boundaries that of the zero averaged density difference. In principle any other choice could be adopted, giving rise to different values of the dipole moment of the sample, and consecutively different value of polarization. As it is shown below, the appropriate treatment of the boundary problem allows us to obtain well defined, physically sound magnitude of the dipole and consequently, the polarization.

IV. POLARIZATION OF BULK AlN, GaN AND InN

In principle, polarization of the system may be obtained from its definition, as the dipole density:

$$\vec{P} = \frac{1}{\Omega} \int d^3r \Delta \rho \vec{r} \quad (2)$$

where Ω is the simulated volume. It was recognized that for electrically neutral systems the result of such procedure does not depend on the choice of the coordinate system, nevertheless it depends on the choice of the simulated area^{4,6,7}.

Another approach was based on division of the ionic and electronic contributions

$$\vec{P} = \vec{P}_{ion} + \vec{P}_{el} \quad (3)$$

where ionic contribution is treated in standard manner using summation over all point charges of the nuclei Ze :

$$\vec{P} = \frac{1}{\Omega} \sum Ze \vec{r} \quad (4)$$

and Berry phase formulation is applied for electronic part, based on linear response theory adiabatic change of the potential, controlled by parameter λ :

$$\vec{P}_{el} = -\frac{2e}{\Omega} \sum_n \int \vec{r} (|w_n^1| - |w_n^0|) d^3r \quad (5)$$

where the sum runs over all occupied real space Wannier functions $|w_n^0\rangle$ and $|w_n^1\rangle$, calculated for both terminations of the adiabatic path (superscripts correspond to $\lambda = 0$ and $\lambda = 1$, respectively) ^{4-7, 49}.

A. Polarization obtained from dipole density

As expected, simulations of finite region should represent the properties of the infinite medium exactly. Standard assumption that periodic boundary conditions are sufficient for this purpose could not be applied to polarized systems. This is because of the uniaxial electric potential difference which prevents the use of periodic boundary conditions. In addition, finite systems could be subjected to arbitrarily selected boundary conditions for potential, giving rise to different field inside. A standard case of a flat parallel plate capacitor demonstrates the dilemma. For the plates uniformly charged, the solution of Poisson equation having zero field outside is routinely selected by invoking additional argument that the potential should be finite at infinity. Formally, the second solution, that of the zero field inside and uniform nonzero field outside, fulfills Poisson equation. Any normalized linear combination of these two solutions equally fulfills Poisson equation. Thus a plethora of the solutions exists, in which an additional argument at infinity is applied to derive physically sound version. This argument could not be applied in the case of finite system embedded in infinite medium, leaving the freedom in selection of any boundary condition for electric potential, i.e. different external field.

In simulation of a finite crystal it is necessary to set zero surface charge in order to prevent additional, spontaneous polarization irrelevant contributions. As there should be no charge or dipole layer at the surfaces, both the electric potential and the electric field are continuous across the system boundaries. In addition, as the modeled sector should be naturally embedded into the infinite medium, the electric potential, the field and its normal derivative should be continuous across the interface, amounting to the following conformity conditions

$$\lim_{\varepsilon \rightarrow 0} \varphi(z = \varepsilon) = \lim_{\varepsilon \rightarrow 0} \varphi(z = -\varepsilon) = \varphi(0) \quad (6)$$

$$\lim_{\varepsilon \rightarrow 0} \vec{E}(z = \varepsilon) = \lim_{\varepsilon \rightarrow 0} \vec{E}(z = -\varepsilon) = \vec{E}(0) \quad (7)$$

$$\lim_{\varepsilon \rightarrow 0} \frac{\partial E_z(z = \varepsilon)}{\partial z} = \lim_{\varepsilon \rightarrow 0} \frac{\partial E_z(z = -\varepsilon)}{\partial z} = \frac{\partial E_z(z = 0)}{\partial z} \quad (8)$$

The considered field could be integrated over the area of the boundary to get average values, which are function of z coordinate only. Since the simulated area can be truncated at any position and the electric field follows the equation:

$$\frac{\partial E_z(z)}{\partial z} = \frac{\rho(z)}{\varepsilon} \quad (9)$$

in which the averaged density profiles, plotted in FIG.1 could be used. Note that the boundary shift should entail appropriate rearrangement of the density distribution. On the other hand in order to model the polarization exactly, it is required that the boundaries of the simulated regions should

represent the surfaces of real crystal, without additional surface charge. Application of the condition (Eqn. 9) to assumption of continuity (Eqn. 8) entails constant density outside the simulated region as shown in FIG. 2. The physically sound approach is that the electronic density difference vanishes outside. Therefore, only the two selected terminations, those plotted by solid lines in FIG. 2, are suitable for calculation of the polarization. It has to be stressed out that this conclusion results from simultaneous requirement that the embedded region is smoothly incorporated into the crystal body and their edge should represent the surface of real crystal without any surface charge.

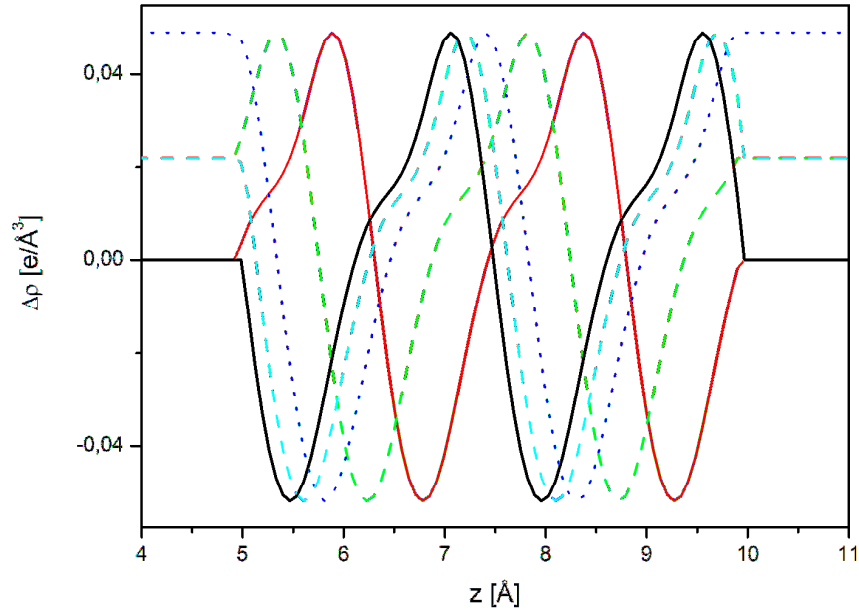


FIG.2. (Color online) Several choices of the truncation of density difference profiles obtained from VASP and its continuation in accordance to the conformity conditions in Eqn. 6,7,8 and 9.

In fact the difference in the selection of the simulated volume directly affects the resulting value of the electric dipole. Using obtained surface averaged electron density difference profiles, the AlN electric dipole magnitude was calculated directly by summation Eqn. 4. The result of these calculations is presented in FIG. 3.

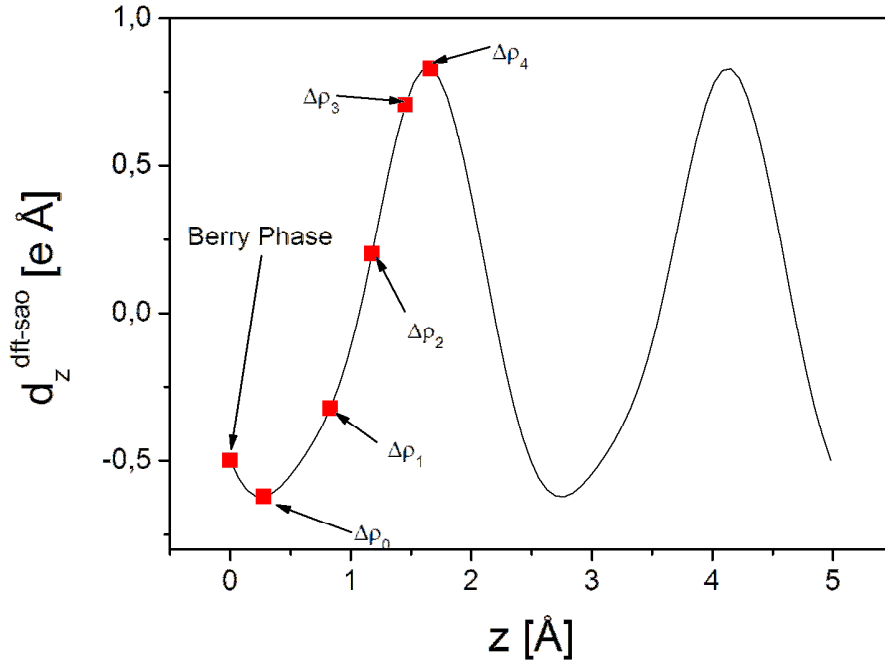


FIG.3. (Color online) Electric dipole of the AlN simulated volume, in function of the shift along c-axis. The results obtained by integration of the profiles truncated in the way presented in FIG. 2 are denoted by red squares.

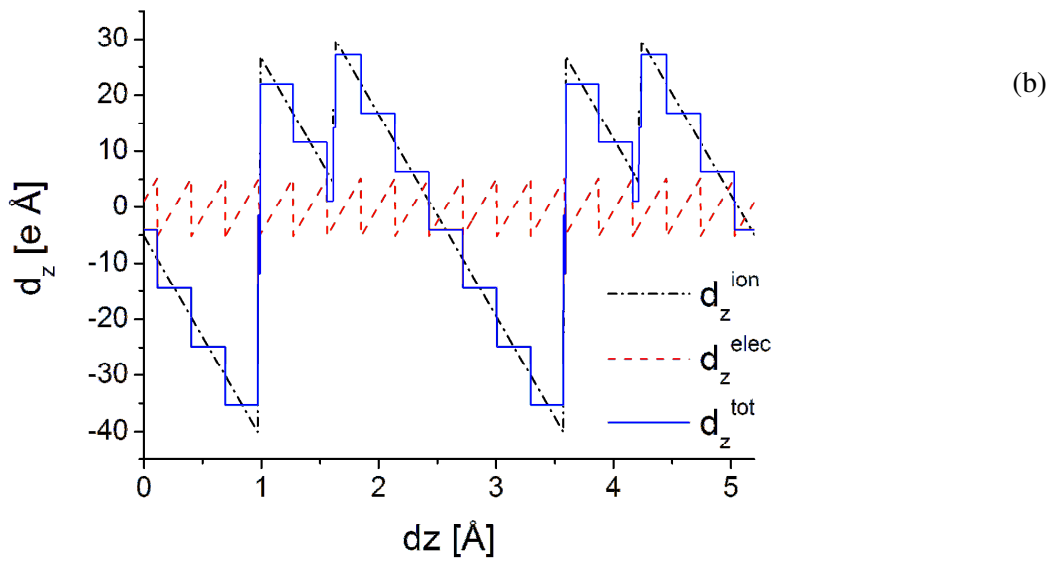
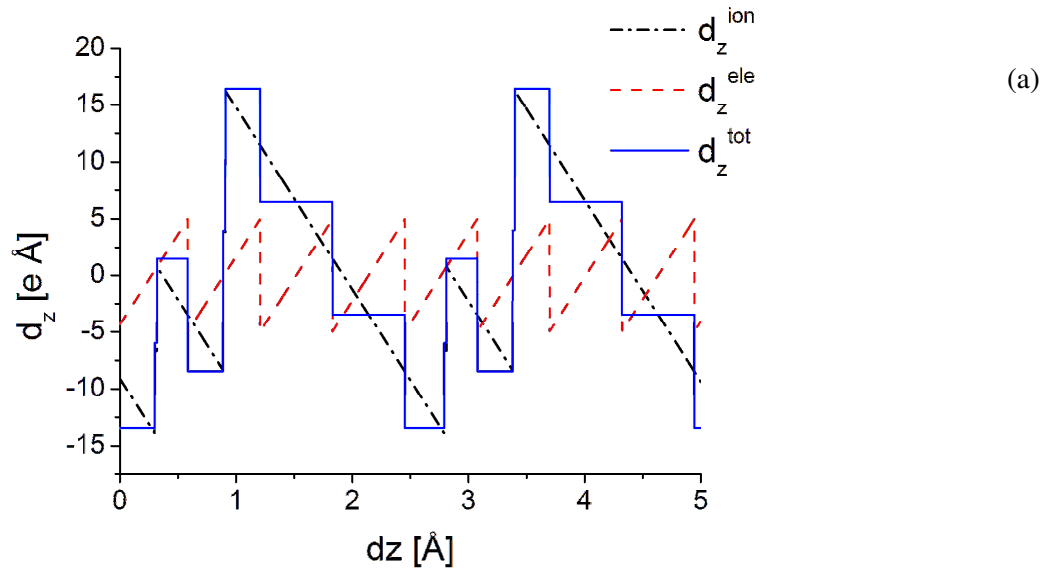
Real crystal selects zero density condition outside. From all possible truncations only the two match, that are denoted by solid lines in FIG. 2. As expected these two selections correspond to maximal and minimal values of the dipole plotted in FIG.3. In fact, these two selections correspond to two possible termination of the top polar surface, i.e. by nitrogen or aluminum atoms. These two cases correspond to the top surface having aluminum triply bonded atoms that are either bare or nitrogen covered. In order to fulfill chemical stoichiometry slab criterion, such change of the top surface and position of the layer of N atoms has to be accompanied by the appropriate rearrangement of the bottom surface. In summary this leads to reversal of the polarization dipole, as shown in FIG. 3.

It has to be noted that the modeled area and the interfaces does not describe the real atomic configuration of any nitride surface. This is a simulation model devised to obtain the polarization and electric field in uniformly polarized nitrides \vec{E}_0 , corresponding to minimal energy of the nitrides under no external field. The magnitude of such field will be determined in the next Section.

B. Polarization obtained from Berry phase formulation

Berry phase formulae for polarization given in Refs 4-7, modified for the application to USPP's and PAW datasets⁴⁷, were calculated using VASP package. In order to obtain good approximation for band gap we have recalculated wavefunctions for PBE charge density with HSE03

functional⁴⁸. Determination of polarization from geometric phase formulation relies on adiabatic change of the crystal potential. Derivation of polarization by Resta is limited to electronic part only². The ionic and electronic contributions, obtained from Eqn. 4 and 5 respectively without assumption of electric neutrality, depend on the coordinate system and the truncation of the integration area.



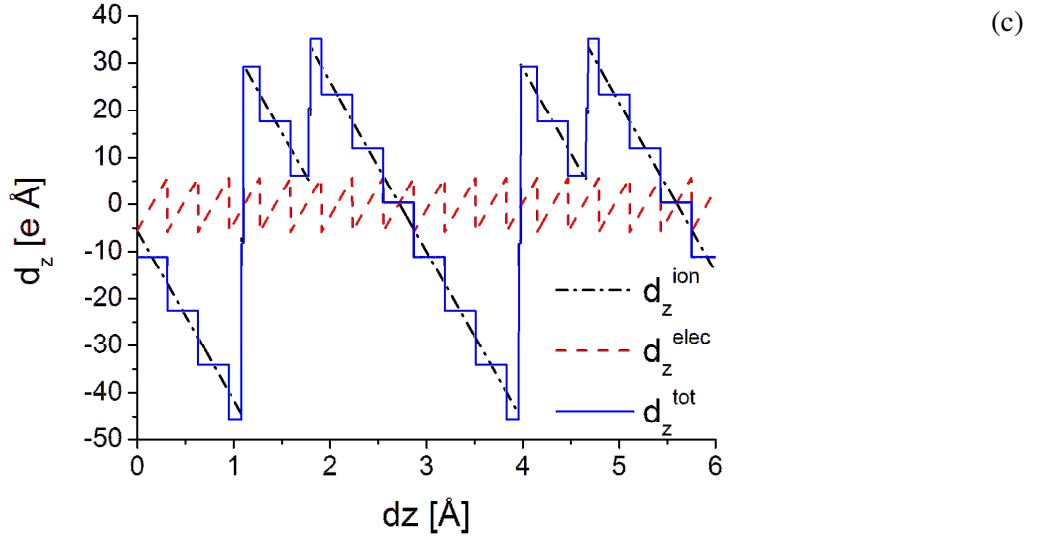


FIG. 4. (Color online) “Z” component of a system dipole as a function of shift along c-axis obtained from Berry phase formulation VASP code: ionic part (Eqn. 4) – black dash-dotted line, electronic part (Eqn. 5) – red dashed line, total – solid blue line; (a) AlN; (b) GaN; (c) InN.

Nevertheless, the combination of both should be independent on the system coordinates, and also on the truncation of the volume. As expected, the ionic contribution is linear function of the z coordinate that undergoes jumps when the N or Ga atoms cross the boundaries. For 4 atoms in total, the same number of jumps in ionic contribution is obtained for all three nitrides equally.

It was also argued that the electronic result is determined modulo periodic change of the geometric phase due to translation of the crystal as a whole, which leads to the following uncertainty:

$$\Delta \vec{P}_{el} = \frac{fe}{\Omega} \sum_n \vec{R}_n \quad (10)$$

where f is the number of the electrons in valence band and R is the lattice period. Accordingly, the number of electrons is: $f = 8$ for AlN, $f = 18$ for GaN and InN, and the number of the jumps follows this prediction⁴. As expected the total polarization being combination of these two contributions is constant but it contains a number of jumps.

It was postulated that the Berry phase results should give the physically meaningful value of polarization by proper selection of the additional constant value given by Eqn. 10 (Ref. 4). This is not as straightforward as it was supposed to be. The number of the possible selection of arbitrary constant is large, even for simple structure of the nitrides. Naturally, the Berry phase result should be within the interval obtained from dipole calculations. This is not the case, but it could be reconciled by additional contribution which may bring the Berry phase result to this interval. In order to compare these results, the obtained polarization values are summarized in TABLE I.

TABLE I. Polarization of nitrides; AlN, GaN and InN, obtained from dipole and Berry phase calculations (in $e/\text{\AA}^2$)

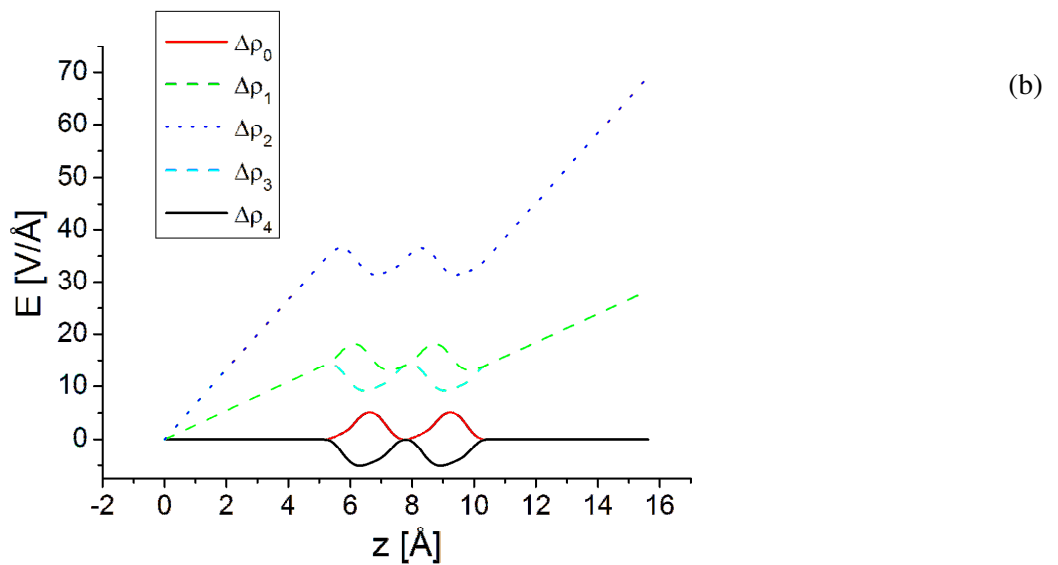
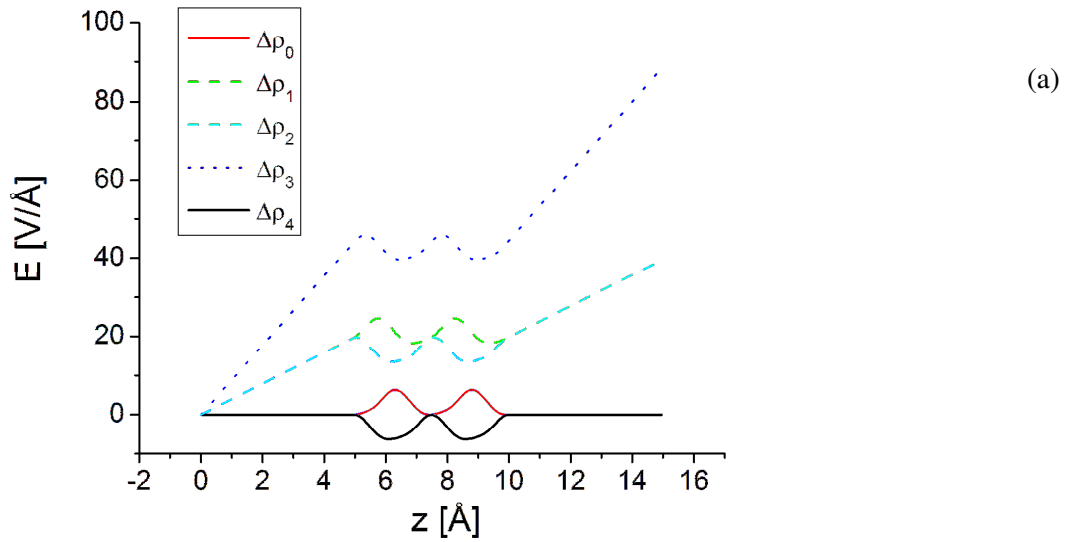
	AlN	GaN	InN
Berry phase	-0.3220	-0.7666	-0.7205
	-0.2028	-0.5404	-0.5386
	-0.1432	-0.3142	-0.3568
	-0.0836	-0.2572	-0.1749
	0.0357	-0.0880	-0.1275
	0.0952	-0.0335	0.0070
	0.1549	0.0250	0.0980
	0.3934	0.1382	0.1889
		0.2513	0.2798
		0.3082	0.3256
		0.3644	0.3708
		0.4774	0.4617
		0.5905	0.5526
$\Delta\rho$	-0.01485	-0.0128	-0.0114
	0.01979	0.0153	0.0123

These polarization values were obtained using the following cell volumes: $\Omega_{\text{AlN}} = 41.79 \text{ \AA}^3$, $\Omega_{\text{GaN}} = 46.03 \text{ \AA}^3$ and $\Omega_{\text{InN}} = 63.30 \text{ \AA}^3$. Using Eqn. 10 and the lattice constants $c_{\text{AlN}} = 4.983 \text{ \AA}$, $c_{\text{GaN}} = 5.206 \text{ \AA}$ and $c_{\text{InN}} = 5.756 \text{ \AA}$, the following additive constants for polarization were obtained: $\Delta P_{\text{el-AlN}} = 0.954 e/\text{\AA}^2$, $\Delta P_{\text{el-GaN}} = 2.036 e/\text{\AA}^2$ and $\Delta P_{\text{el-InN}} = 1.637 e/\text{\AA}^2$. These values are relatively high compared to the dipole results obtained with method based on density difference Eqn. 1. It is worth mentioning that the jumps in the electronic part follow Eqn. 10 for $f = 1$, i.e. accounting single electron contribution only. Such jumps could be translated into the following additional constant values: $\Delta P_{\text{el-AlN-1}} = 0.1192 e/\text{\AA}^2$, $\Delta P_{\text{el-GaN-1}} = 0.1131 e/\text{\AA}^2$ and $\Delta P_{\text{el-InN-1}} = 0.0909 e/\text{\AA}^2$. In fact these polarization values obtained in dipole model may be approximated by appropriate subtraction of single electron values.

Notably, the nitrides spontaneous polarization obtained by Bernardini et al.¹¹ using Berry phase approach were: AlN: -0.081 C/m^2 ($-5.05 \times 10^{-3} e/\text{\AA}^2$), GaN: -0.029 C/m^2 ($-1.81 \times 10^{-3} e/\text{\AA}^2$), and InN: -0.032 C/m^2 ($-1.99 \times 10^{-3} e/\text{\AA}^2$). These results are slightly lower than our results obtained from dipole calculations. Additional difference stems from the fact that, the dipole formulation presented above, gives two different polarization values.

V. POLARIZATION INDUCED FIELD IN BULK AlN, GaN AND InN.

In addition to the polarization, the physically relevant quantity, directly affecting the performance of MQW based devices, is polarization induced electric field. As it was argued above, the field may be obtained modulo additional value. In fact, this freedom is used in solution of Poisson equation by FFT method. Nevertheless, the physically sound solution is found using the same criterion as for capacitor with zero field at infinity. This solution was obtained for zero density outside, i.e. for the two selected cases above. This formulation allows obtaining the two possible values of the field, which corresponds to two selection of the crystal termination. In FIG. 5, the electric fields obtained for selected cases shown in FIG.2. The physically sound solutions are plotted using solid lines.



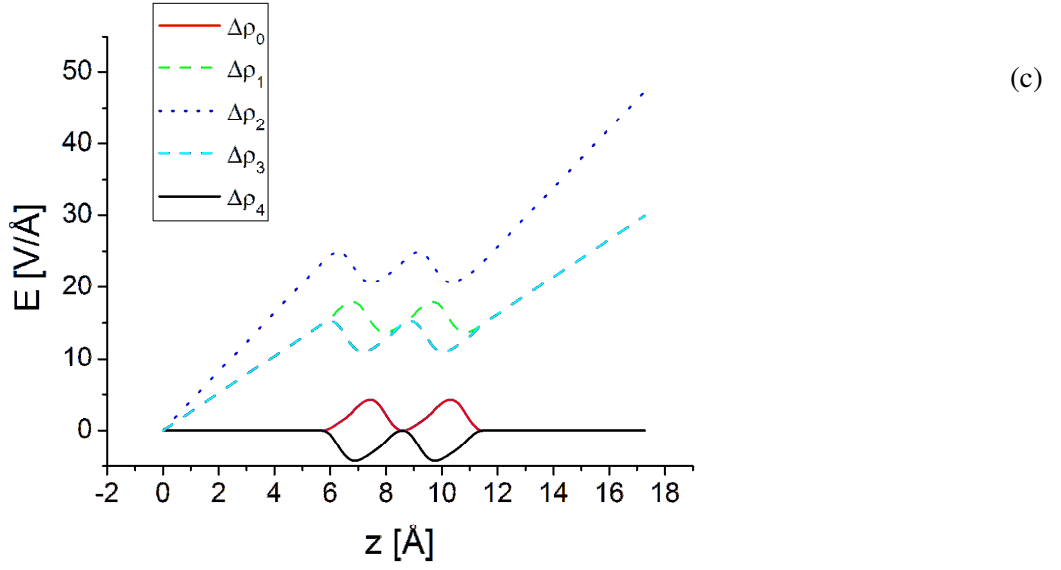
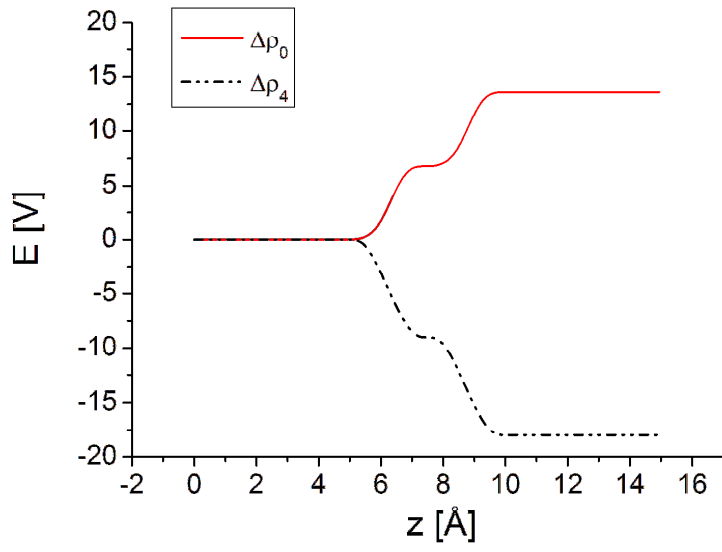
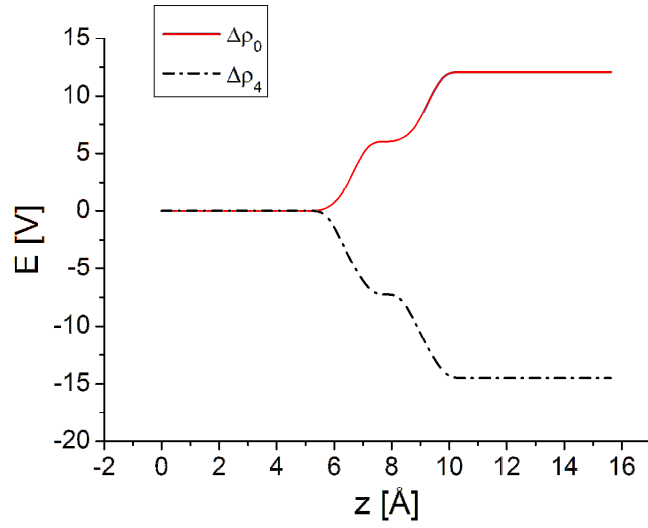


FIG. 5. (Color online) Area averaged electric field plotted, along c-axis, in single periodic cell of: (a) AlN; (b) GaN; (c) InN.

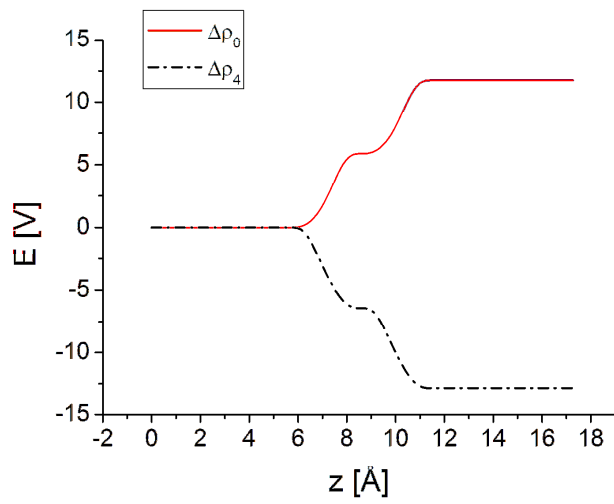
In addition, FIG. 6 presents the physically sound electric potential distributions plotted for AlN, GaN and InN. From these potential distributions the following potential differences were obtained: for AlN: $\Delta V_{\text{AlN}}^{\text{N}} = -18.00 \text{ V}$ and $\Delta V_{\text{AlN}}^{\text{Al}} = 13.59 \text{ V}$; for GaN: $\Delta V_{\text{GaN}}^{\text{N}} = -14.49 \text{ V}$ and $\Delta V_{\text{GaN}}^{\text{Ga}} = 12.06 \text{ V}$; for InN: $\Delta V_{\text{InN}}^{\text{N}} = -12.85 \text{ V}$ and $\Delta V_{\text{InN}}^{\text{In}} = 11.75 \text{ V}$. Since the following lattice constants were adopted for the modeling: $c_{\text{AlN}} = 4.983 \text{ \AA}$, $c_{\text{GaN}} = 5.206 \text{ \AA}$ and $c_{\text{InN}} = 5.756 \text{ \AA}$, the average fields are as follows: for AlN: $E_{0,\text{AlN}}^{\text{N}} = -3.612 \text{ V/\AA}$ and $E_{0,\text{AlN}}^{\text{Al}} = 2.727 \text{ V/\AA}$; for GaN: $E_{0,\text{GaN}}^{\text{N}} = -2.783 \text{ V/\AA}$ and $E_{0,\text{GaN}}^{\text{Ga}} = 2.317 \text{ V/\AA}$; for InN: $E_{0,\text{InN}}^{\text{N}} = -2.232 \text{ V/\AA}$ and $E_{0,\text{InN}}^{\text{In}} = 2.041 \text{ V/\AA}$. These values are relatively high and they should be relatively easy to detect in nitride based structures. Note that screening could decrease or remove its influence, in the case when the size of the structures is comparable or larger than the characteristic screening lengths.



(a)



(b)



(c)

FIG. 6. (Color online) Area averaged electric potential plotted, along c-axis, in single periodic cell of: (a) AlN; (b) GaN; (c) InN. Black (solid) and red (broken) lines correspond to two different possible electric field directions, related to different polarization values.

These fields are to be used from in any geometrical arrangement of nitrides, encountered in electronic or optoelectronic devices by minimization of the electrostatic energy functional:

$$\Delta W = \int d^3r \frac{\epsilon (\vec{E} - \vec{E}_0)^2}{2} \quad (11)$$

Naturally, the uniform polarization field \vec{E}_0 is the minimal energy solution, corresponding to uniform polarization in the single finite size crystal without any surface or external contributions. These fields are the maximal field induced in finite size polarized semiconductors. In any real quantum structure, the fields should be lower, nevertheless that should affect properties of these structures considerably.

VI. SUMMARY

Two different approaches to polarization of nitride semiconductors were assessed, and the conclusions were used to development of these models. It was shown that Berry phase formulation of the electron related polarization component provides a number of various solutions, different for various selection of the simulated volume. The electronic part gives saw-like pattern for polarization. A total number of these solutions, related to well known scaling of the geometric phase is equal to the number of valence electrons in the system. Summed with similar pattern for ionic part, provides several polarization values.

Standard dipole density formulation depends on the selection of the simulation volume in periodic continuous way. Using the condition of continuous embedding into the infinite medium, and simultaneously, the zero surface charge representation at crystal boundary, physically sound solution could be identified. This solution corresponds to maximal and minimal polarization values and corresponds to different physical termination of the crystal surfaces, either bare or covered by complementary atoms. This change leads to polarization and electric field reversal. Values of the fields are maximal values possible for finite size polarized nitrides without any surface charges or external fields.

ACKNOWLEDGEMENTS

The calculations reported in this paper were performed using computing facilities of the Interdisciplinary Centre for Modelling of Warsaw University (ICM UW). The research was partially supported by the European Union within European Regional Development Fund, through grant Innovative Economy (POIG.01.01.02-00-008/08).

REFERENCES

- ¹ L.D. Lanadau, and E.M. Lifsic, *Electrodynamics of Continuous Media* (Pergamon, Oxford, 1984).
- ² R. Resta, *Rev. Mod. Phys.* **66**, 899 (1994).
- ³ R. Resta, *Ferroelectrics* **136**, 51 (1992).
- ⁴ R. M. Martin, *Phys. Rev. B* **9**, 1998 (1974).
- ⁵ R. D. King-Smith, and D. Vanderbilt, *Phys. Rev. B* **47** 1651 (1993).
- ⁶ D. Vanderbilt, and R.D. King-Smith, *Phys. Rev. B* **48** 4442 (1993).
- ⁷ R. Resta, in *Berry Phase in Electronic Wavefunctions, Troisième Cycle de la Physique en Suisse Romande*, (Année Academique, 1996).
- ⁸ M. Posternak, A. Baldereschi, A. Catellani, and R. Resta, *Phys. Rev. Lett.* **64** 1777 (1990).
- ⁹ A. K. Tagantsev, *Phys. Rev. Lett.* **69** 389 (1992).
- ¹⁰ M. E. Lines, and A.M. Glass, *Principles and Applications of Ferroelectrics and Related Materials*, (Clarendon, Oxford, 1974)
- ¹¹ F. Bernardini, V. Fiorentini, and D. Vanderbilt, *Phys. Rev. Lett.* **79**, 3958 (1997)
- ¹² F. Bernardini, V. Fiorentini, D. Vanderbilt, *Phys. Rev. B* **56**, R10024 (1997).
- ¹³ F. Bernardini, V. Fiorentini, *Phys. Stat. Solidi B* **216**, 391 (1999).
- ¹⁴ M. P. Halsall, J. E. Nicholls, J. J. Davies, B. Cockayne, and P.J. Wright, *J. Appl. Phys.* **71**, 907 (1992).
- ¹⁵ M. Buongiorno Nardelli, K. Rapcewicz, and J. Bernholc, *Appl. Phys. Lett.* **71**, 3135 (1997).
- ¹⁶ S. P. Łepkowski, H. Teissyere, T. Suski, P. Perlin, N. Grandjean, J. Massies, *Appl. Phys. Lett.* **79**, 1483 (2001).
- ¹⁷ T. Takeuchi, C. Wetzel, S. Yamaguchi, H. Sakai, H. Amano, I. Akasaki, Y. Kaneko, S. Nakagawa, Y. Yamaoka, and N. Yamada, *Appl. Phys. Lett.* **73**, 1691 (1998).
- ¹⁸ R. Langer, J. Simon, V. Ortiz, N. T. Pelekanos, A. Barski, R. Ander, and M. Godlewski, *Appl. Phys. Lett.* **74**, 3827 (1999).
- ¹⁹ I. J. Seo, H. Kollmer, J. Off, A. Sohmer, F. Scholz, and A. Hangleiter, *Phys. Rev. B* **57**, R9435 (1998).
- ²⁰ P. Lefebvre, J. Allegre, B. Gil, H. Mathieu, N. Grandjean, M. Leroux, J. Massies, and P. Bigenwald, *Phys. Rev. B* **59**, 15363 (1999).
- ²¹ Y. C. Shen, G. O. Muller, S. Watanabe, N. F. Gardner, A. Munkholm, and M. R. Kramers, *Appl. Phys. Lett.* **91**, 141101 (2007).
- ²² I. V. Rozhansky, and D. A. Zakeheim, *Phys. Stat. Solidi C* **3**, 2160 (2006).
- ²³ M. F. Schubert, S. Chajed, J. K. Kim, E. F. Schubert, D. D. Koleske, M. F. Crawford, S. R. Lee, A. J. Fisher, G. Thaler, and M. A. Banas, *Appl. Phys. Lett.* **91**, 231114 (2007).
- ²⁴ J. Xie, X. Ni, Q. Fan, R. Schimada, U. Ozgor, and H. Morkoc, *Appl. Phys. Lett.* **93**, 121107 (2008).

- ²⁵ H. Teisseyre, A. Kaminska, G. Franssen, A. Dussaigne, N. Grandjean, I. Grzegory, B. Lucznik, and T. Suski, *J. Appl. Phys.* **105**, 63104 (2009).
- ²⁶ H. Morkoc, *Handbook of Nitride Semiconductors and Devices* (Wiley-VCH, Berlin, 2008), vol. 3.
- ²⁷ G. Kresse, and J. Hafner, *Phys. Rev. B* **47**, 558 (1993); *ibid.* **49**, 14 251 (1994).
- ²⁸ G. Kresse, and J. Furthmüller, *Comput. Mat. Sci.* **6** 15 (1996).
- ²⁹ G. Kresse, and J. Furthmüller, *Phys. Rev. B* **54**, 11169 (1996).
- ³⁰ P. Ordejón, D. A. Drabold, M. P. Grumbach, and R. M. Martin, *Phys. Rev. B* **48**, 14646 (1993).
- ³¹ P. Ordejón, D. A. Drabold, M. P. Grumbach, and R. M. Martin, *Phys. Rev. B* **51**, 1456 (1995).
- ³² J. M. Soler, E. Artacho, J. D. Gale, A. García, J. Junquera, P. Ordejón, and D. Sánchez-Portal, *J. Phys.: Condens. Matter* **14**, 2745 (2002).
- ³³ B. J. Delley, *J. Chem. Phys.* **92**, 508 (1990); *ibid* **113**, 7756 (2000).
- ³⁴ S. P. Łepkowski, and J. A. Majewski, *Phys. Rev. B* **74** 35336 (2006).
- ³⁵ H.J Monkhorst, and J. D. Pack, *Phys. Rev. B* **13** 5188 (1976).
- ³⁶ J. P. Perdew, K. Burke, and M. Ernzerhof, *Phys. Rev. Lett.* **77** 3865 (1996).
- ³⁷ P.E. Blöchl, *Phys. Rev. B* **50** 17953 (1994).
- ³⁸ G. Kresse, and J. Joubert, *Phys. Rev. B* **59** 1758 (1999).
- ³⁹ N. Troullier, and J. L. Martins, *Phys. Rev. B* **43**, 1993 (1991), *ibid* **43**, 8861 (1991).
- ⁴⁰ Z. Wu, and R.E. Cohen, *Phys. Rev. B* **73** 235116 (2006).
- ⁴¹ C. C. Roothaan, *J. Rev. Mod. Phys.* **32**, 179 (1960); *ibid* **23**, 69 (1951).
- ⁴² A. D. Becke, *J. Chem. Phys.* **88**, 2547 (1988).
- ⁴³ C. Lee, W. Yang, and R. G. Parr, *Phys. Rev. B* **37**, 785 (1988).
- ⁴⁴ T. Tsuneda, T. Suzumura, and K. Hirao, *J. Chem. Phys.* **110**(22), 10664 (1999).
- ⁴⁵ B. Delley, *J. Phys. Chem.* **100**, 6107 (1996).
- ⁴⁶ E. P. Ewald, *Ann. Phys.* **64**, 253 (1921).
- ⁴⁷ D. Vanderbilt, and R. D. King-Smith, in *Electronic polarization in the ultrasoft pseudopotential formalism* (Unpublished report, 1998).
- ⁴⁸ J. Heyd, G. E. Scuseria, and M. Ernzerhof, *J. Chem. Phys.* **118**, 8207 (2003).
- ⁴⁹ R.W. Nunez, and X. Gonze, *Phys. Rev. B* **63** 115107 (2001).